Enhanced TiO$_2$ photocatalysis by Cu in hydrogen production from aqueous methanol solution

Nae-Lih Wu*, Min-Shuei Lee

Department of Chemical Engineering, National Taiwan University, Taipei 106, Taiwan

Abstract

Cu particles have been deposited on TiO$_2$ by incipient-wetness impregnation followed by low-temperature (400°C) calcination/reduction, and the metallization process leads to significant enhancement in photocatalytic activity of TiO$_2$ for H$_2$ production from aqueous methanol solution. The activity exhibits up to 10-fold enhancement at the optimum loading of $\sim$ 1.2 wt% Cu. Spectroscopic studies indicated that the Cu particles were oxidized during reaction to have a valence lower those of thermally oxidized particles, which showed inferior activities. Dissolution of Cu ion in TiO$_2$ lattice, in contrast, resulted in reduction in photocatalytic activity.
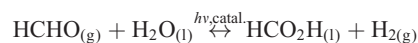
1. Introduction

Photocatalytic production of hydrogen using sunlight as the energy input is a valuable sustainable-energy technology. In this case, solar energy is stored by driving chemical reactions "up-hill" toward chemicals, such as H$_2$, of higher chemical potentials. Due to its high stability against photo-corrosion and its favorite electronic energy band structure, TiO$_2$ has drawn tremendous attention for such applications. For H$_2$ production from water, many studies have concluded that direct splitting of water into H$_2$ and O$_2$ has a very low efficiency due to rapid reverse reaction. A much higher hydrogen production rate can be obtained by addition of the "so-called "sacrificial reagents," such as alcohols and other organics [1–4], which are oxidized to products that are less reactive toward hydrogen. For H$_2$ production from a water/methanol (MeOH) solution, depending on reaction conditions and on whether metal catalyst used, the reaction could proceed either stepwise,
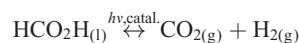
involving stable intermediates, such as aldehydes and acids:

$$\text{MeOH}_{(l)} \overset{hv, \text{catal.}}{\Longleftrightarrow} \text{HCHO}_{(g)} + \text{H}_{2(g)}$$

$$\Delta G_1^\circ = 64.1 \text{ kJ/mol [5]}, \tag{1}$$

$$\text{HCHO}_{(g)} + \text{H}_2\text{O}_{(l)} \overset{hv, \text{catal.}}{\Longleftrightarrow} \text{HCO}_2\text{H}_{(l)} + \text{H}_{2(g)}$$

$$\Delta G_2^\circ = 47.8 \text{ kJ/mol}, \tag{2}$$

$$\text{HCO}_2\text{H}_{(l)} \overset{hv, \text{catal.}}{\Longleftrightarrow} \text{CO}_{2(g)} + \text{H}_{2(g)}$$

$$\Delta G_3^\circ = -95.8 \text{ kJ/mol}, \tag{3}$$

as suggested by Sakata et al. [1–4], or in one-step on catalyst surface to give the overall reaction:

$$\text{MeOH}_{(l)} + \text{H}_2\text{O}_{(l)} \overset{hv, \text{catal.}}{\Longleftrightarrow} \text{CO}_{2(g)} + 3\text{H}_{2(g)}$$
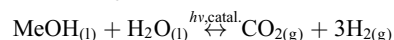
$$\Delta G^\circ = 16.1 \text{ kJ/mol}, \tag{4}$$

as suggested by Chen et al. [6]. H$_2$ is produced in all of these steps.

Deposition of Pt-group metals, including Ni, Pd and Pt, on TiO$_2$ has been shown to greatly enhance the photocatalytic production of H$_2$ from either pure water or water/sacrificial reagent solutions. Sakata et al. [4] attributed the enhancement to the catalytic effects of the metal particles on H$_2$

---

*Corresponding author. Tel.: +886-2-23627158; fax: +886-2-23623040.

E-mail address: nlw001@ntu.edu.tw (N.-L. Wu).

evolution. Bowker et al. [7], on the other hand, suggested that the presence of Pd provides a reaction pathway which involves chemisorption and dehydrogenation of MeOH on Pd to produce chemisorbed CO and subsequent oxidation of the chemisorbed CO to CO_2.

Cu-containing TiO_2 catalysts are well known for their photocatalytic activity toward CO_2 reduction [8–11] but much less is known for its performance in H_2 production from water/alcohol solution, except in one case where a Cu–TiO_2 catalyst was reported to exhibit enhanced H_2 production from a water/MeOH solution with photon energies within the visible-light region [12]. In that particular study, the photocatalyst was synthesized by calcining a mixture of $Ti(SO_4)_2$ and $Cu(NO_3)_2$ (1 wt% of CuO) at 930 K, and it exhibited enhanced absorption within the visible light range, in accompanied with increased catalytic activity, upon Xe lamp irradiation. Cu could be either dissolved in TiO_2 lattice or deposited as individual particles on the TiO_2 surface. No attempt was made therein to distinguish their roles in the enhancement effect.

In this work, Cu particles were deposited on TiO_2 via an incipient-wetness impregnation method followed by low-temperature (400°C) calcination in order to minimize Cu dissolution into the oxide lattice, and its photocatalytic activity toward H_2 production from a water/MeOH solution was investigated. It is shown that the deposited Cu particles, which are in the oxidized state during reaction, cause up to 10-fold enhancement in H_2 production. In contrast, dissolution of Cu ion in TiO_2 lattice exhibited negative effect.

2. Experimental

TiO_2 powder was synthesized by a conventional sol–gel process. $TiCl_4$ was first dissolved in an ethanol/water (volume ratio = 4 : 1) solution, and ammonia was then introduced into the solution to induce condensation until pH reached 7.5. The resulted gelatinous precipitate was filtered and washed to reduce $[Cl^-]$ to below 5×10^{-4} M, as determined by ion chromatography, and then dried at 65°C in air. Cu was loaded by an incipient-wetness method, in which an aqueous solution containing $CuCl_2 \cdot 2H_2O$ was added to the oxide powder in an amount that was just sufficient to wet completely the powder. The resulted powder was then dried and calcined in synthetic air (N_2/O_2 mol ratio = 79 : 21) to make the catalyst. The standard calcination procedure involved purging the reactor with the gas for 1 h, heating the powder at a rate of 100°C/h to 400°C, and holding the powder at 400°C for 1 h before finally the powder being furnace-cooled. The catalyst powders were stored as calcined, and they were further reduced at 400°C by H_2 (3 mol% in N_2) for 3 h prior to characterization works, including the spectroscopic and kinetic analyses.

Kinetic experiments were carried out by using a vertical tubular batch reactor made of quartz. During a typical run, the entire reactor was enclosed inside a UV-light house (Rayonet photochemical reactor, RPR-100), and the reactor was half-filled with a water/MeOH (volume ratio=1.4:1) solution, in which the oxide particles, in an amount of 1.25 g/l, were constantly dispersed by a magnetic stirrer. The light house was equipped with 16 UV-light (maximum intensity at 300 nm) tubes, each having a power of 12 W. The unfilled space above the solution was evacuated at the beginning of reaction, and H_2 concentration was measured intermittently by extracting a small volume of the gas-phase product for gas chromatography analysis. The accumulative H_2 production data were then calculated from the concentration data, assuming ideal-gas behavior.

X-ray diffraction (XRD; Mac-Science/ MXP3) was employed to determine the crystalline phase and grain size of the TiO_2 powders, and the average crystallite size was calculated by using the Debye–Scherrer equation. The surface area was determined by N_2 adsorption. X-ray photoelectron spectroscopic (XPS) analysis was carried out on a spectrometer (MT 500, VG Microtech) equipped with a Mg (Kα) X-ray source. Before being put into the XPS vacuum chamber, the freshly reduced powders were exposed to air for less than 8 h, an exposure period similar to that during the kinetic experiments. Diffuse reflectance ultraviolet–visible (UV–VIS) spectroscopic analysis was conducted on a Hitachi U3410 spectrometer, which is equipped with an integration sphere and PbS and photomultiplier detectors for photon detection. Deuterium and tungsten iodide lamps are used as the light sources for wavelength ranges of 185–340 and 340–2500 nm, respectively. The spectra were acquired at room temperature with $BaSO_4$ as the reference.

3. Results and discussion

The blank TiO_2 catalyst (Cu loading = 0 wt%) appeared yellowish, and XRD analysis indicated the presence of only the anatase phase with an average grain size of 9.0 nm, based on the (1 0 1) reflection. The yellowish color, which can be removed by annealing in oxygen above 500°C, is believed to be caused by oxygen vacancies. The BET surface area is 110 m/g. With increasing Cu deposition up to a maximum loading of 1.9 wt% Cu, the catalysts turned increasing reddish. XRD, however, did not detect reflection of Cu, presumably because of the combination of its low content and small particle sizes. The grain size of TiO_2, being insensitive to the Cu content, was slightly increased to ∼10.0 nm, presumably caused by additional reduction heat treatment.

UV–VIS spectroscopic analysis (Fig. 1) of the blank TiO_2 showed a major UV-absorption near 350 nm wavelength and a minor one near 450 nm. The latter is consistent with its yellowish appearance. Determined by Tauc plot [$(\alpha h v)^2$ versus hv, where α is the absorbance] (Fig. 1, the inset) [13–15], the major absorption edge energy is 3.15 eV, close to the theoretical value (3.20 eV) of anatase TiO_2. Deposition of Cu caused a reduction in major edge energy to 3.09 eV and a dramatic increase in visible-light absorption. The
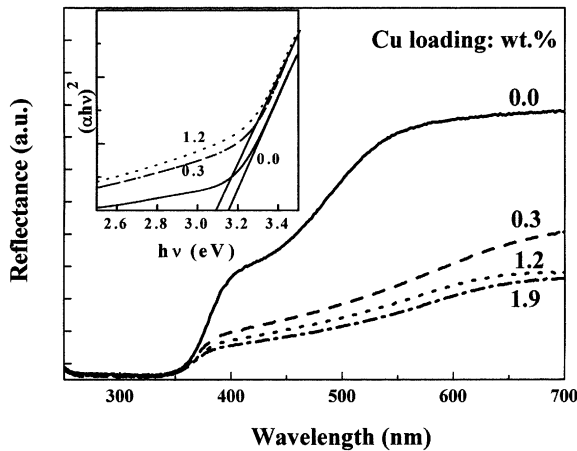
Fig. 1. Diffuse reflectance spectra of TiO_2 catalysts. The lines are indexed according to Cu loading (wt%). The inset shows the $(\alpha h\nu)^2$ versus $h\nu$ plots, where α is absorbance.
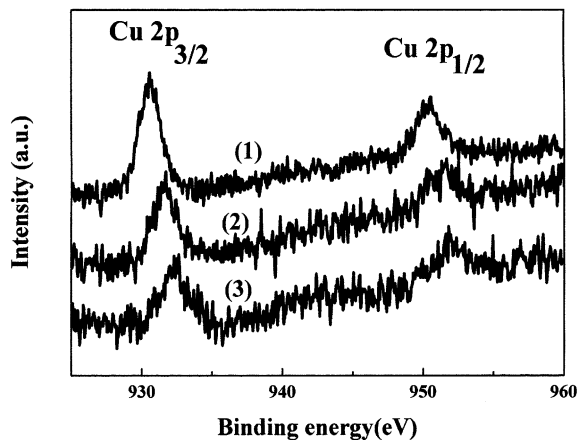

Fig. 2. Cu ($2p_{3/2}$ and $2p_{1/2}$) XPS spectra of the catalysts subjected to (1) reduction, (2) H_2 production reaction, and (3) oxidation in air at room temperature for 120 h, respectively.
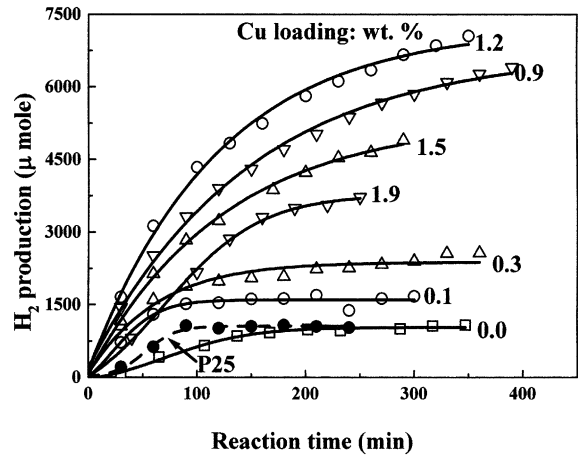

Fig. 3. H_2 generation curves. The data sets are indexed by their Cu loading (wt%), while the commercial catalyst is indexed as P25. The lines are fitted with Boltzman equation.

absorption extends up to 700 nm in wavelength, which is consistent with their reddish appearance, and the absorbance increased with increasing Cu content. XPS analysis carried out on the 1.2% Cu-deposited catalysts detected only Cu, Ti, O, and C, and no Cl peak was observed. The Cl associated with the Cu source, $CuCl_2 \cdot 2H_2O$, may be removed by reaction with hydrogen during reduction. This reaction was confirmed by temperature-programmed reduction experiment using $CuCl_2 \cdot 2H_2O$ powder. The detected Cu ($2p_{3/2}$) binding energy (930.5 eV; Fig. 2) is lower than that of any known oxidized Cu species, suggesting that oxidation of the Cu surface is very limited prior to the photocatalytic reaction. Quantitative analysis [16] considering only the first three elements gave a Cu content of 1.20 (± 0.02) wt%,

suggesting that Cu was indeed largely on the TiO_2 surface, rather than embedded within the TiO_2 matrix.

For the kinetic study, a small amount of H_2 was detected from the solution even without the catalyst. Nevertheless, H_2 production was greatly enhanced with the presence of the catalysts. Fig. 3 summarizes the H_2-generation curves for catalysts of different Cu loading. In all cases, upon UV-irradiation, H_2 was produced at steadily increasing concentration with time until it saturated at a steady level. The saturation is not due to de-activation of the catalyst but because of equilibrium, i.e., the balance between forward and reverse reaction rates. It was shown that, after the system was evacuated during the saturation period to completely remove the gaseous species and then sealed, essentially the same H_2 generation curve was subsequently obtained. As the reactor configuration is far from optimum, no emphasis should be placed on the absolute quantum efficiency of the catalysts. Rather, they can be compared relative to the performance under the same reaction conditions of a commercial TiO_2, Degussa P25 (Fig. 3), which has widely been employed in the literature.

All the generation curves can be satisfactorily fitted by the Boltzman equation, having a form of

$$P = P_{eq} + (A - P_{sat})/\{1 + \exp[(t - t_0)/\delta]\},$$

where P is the accumulative hydrogen production (in μmol) within the open space in the reactor, P_{sat}, the equilibrium (i.e., saturation) accumulative production, t, the reaction time (in min), and A, t_0, and δ are parameters. Mathematically, this equation gives a curve containing an inflection point at t_0. For $t_0 > 0$, the maximum hydrogen generation rate, $dP/dt|_{max}$, occurs at this inflection point. For $t_0 \leqslant 0$, however, it means in reality that the maximum rate occurs at the very beginning of the reaction. The fitted $dP/dt|_{max}$ and P_{eq} data are summarized in Fig. 4. They were found to
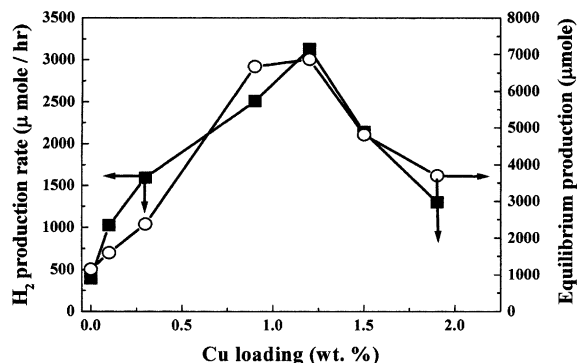
Fig. 4. Effect of Cu loading (wt%) on H_2 production rate and equilibrium production.

Fig. 5. Effect of Cu oxidation on H_2 production. Key: (1) oxidation in situ by reaction; (2) thermal oxidation at 400°C in air for 1 h; (3) thermal oxidation in air at room temperature for 120 h. Cu loading is the same (1.2 wt%).

follow the same trend against Cu loading, both showing a maximum at 1.2 wt% Cu. The maximum production rate, $dP/dt|_{max}$, at the optimum Cu content is 10 times that of the blank TiO_2 and 4.5 times that of the P25 catalyst..

Compared with the commercial P25 catalyst, the blank TiO_2 synthesized in this study has a lower maximum production rate but eventually reaches about the same saturation level (Fig. 3). The latter suggests that the blank TiO_2 provides also a slower reverse reaction. Deposition of Cu particles shows enhancement not only in the maximum production rate but also in the saturation level, suggesting that the Cu catalyst accelerates the forward reaction to a greater extent than the reverse one. The occurrence of an optimum metal loading has also been observed for Pd-deposited TiO_2 catalyst [7], and it is indicative of interfacial active sites at and/or near the peripheries of the Cu particles. The total peripheral length first increases with increasing Cu particle number and size until reactive domains begin to overlap. Further increase in Cu loading would only lead to reduction of the peripheral length, and hence to lower reactivity.

It was also noticed that the catalysts, which appeared reddish at the beginning of the reaction, turned greenish after reaction, suggesting oxidation of Cu. This was confirmed by XPS (Fig. 2), which showed an increase by 1 eV in Cu ($2p_{3/2}$) binding energy to $\sim$931.5 eV. The result indicated that it is an oxidized Cu species that is active. Two types of oxidized Cu–TiO_2 catalysts (1.2 wt% of Cu) were thus prepared for comparison. Following the standard thermal reduction procedure, the first one was oxidized by prolonged (5 days) exposure in air at room temperature, while the second one was heated in air at 400°C for 1 h. Both catalysts did show significant photocatalytic activities (Fig. 5) but were inferior to the one oxidized during the reaction. XPS showed that Cu in these two catalysts exhibited higher binding energies, hence higher valences than that oxidized in situ during the reaction. The Cu ($2p_{3/2}$) binding energy (932.3 eV) for the catalyst oxidized at room temperature (Fig. 2) is consistent with Cu^{+1} in Cu_2O, and
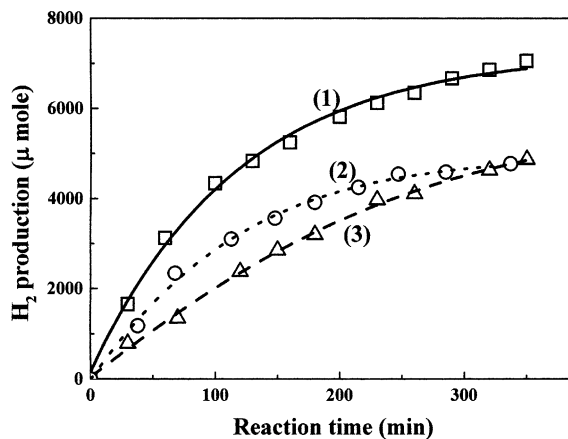
therefore the Cu in the reaction-oxidized catalyst has an average valence between 0 and $+1$.

In order to illustrate the effect of Cu dissolution, as opposed to Cu deposition, a different batch of Cu-containing (1.2 wt%) catalyst was prepared by mixing the Cu and Ti sources, namely $CuCl_2$ and $TiCl_4$, at the very beginning of the synthesis process, an approach similar to that adopted in Ref. [12]. After the same thermal calcination and reduction procedures, XPS analysis of this catalyst showed a Cu content of 1.06 ($\pm$0.02) wt%, indicating that part of the Cu introduced is not on the surface of TiO_2. As the sol–gel process allows for mixing in the molecular scale, it is believed that some Cu does dissolve in the oxide lattice. Accordingly, for brevity, this catalyst will be referred to as the "Cu-doped" catalyst. As shown in Fig. 6, the H_2 production activity of the doped catalyst is lower than that achieved by Cu-deposition either with the same overall loading (1.2 wt%) or with about the same "surface loading" ($\sim$1.0 wt%). The latter may suggest that Cu-doping within the TiO_2 lattice has a negative effect on the overall catalytic activity.

In summary, deposition with Cu particles was found to greatly enhance the photocatalytic activity of TiO_2 toward H_2 production from aqueous methanol solution. The Cu particles were oxidized and self-regulated to achieve the optimum valence for maximum activity during the course of reaction. On the other hand, doping with Cu ions in TiO_2 lattice was found to reduce the activity.
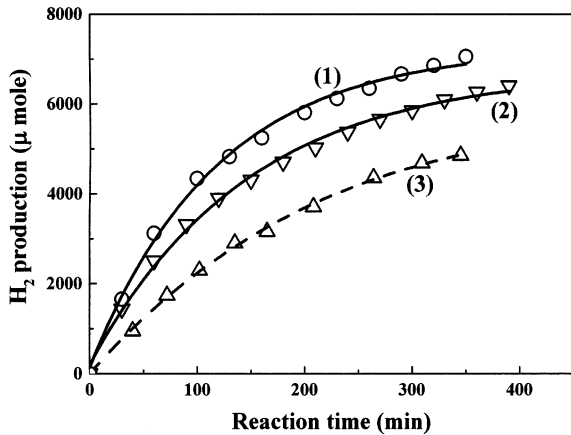
Acknowledgements

Fig. 6. Effect of Cu loading method on H_2 production. Key: (1) and (2) incipient-wetness method with 1.2 and 0.9 wt%, respectively; (3) doping method with 1.2 wt%.

References

[1] Kawai T, Sakata T. Photocatalytic hydrogen production from liquid methanol and water. JCS Chem Commun 1980;694–5.

[2] Kawai T, Sakata T. Photocatalytic hydrogen production from water by the decomposition of poly-vinylchloride, protein, algae, dead insects, and excrement. Chem Lett 1981;81–4.

[3] Sakata T, Kawai Y. Heterogeneous photocatalytic production of hydrogen and methane from ethanol and water. Chem Phys Lett 1981;80:341–4.

[4] Sakata T, Kawai T, Hashimoto K. Photochemical diode model of Pt/TiO2 particle and its photocatalytic activity. Chem Phys Lett 1982;88:50–4.

[5] Lide DR, editor. Handbook of Chemistry and Physics, 83rd ed. Boca Raton, FL: CRC press; 2002. pp. 5.1–.60.

[6] Chen J, Ollis DF, Rulkens WH, Bruning H. Photocatalyzed oxidation of alcohols and organochlorides in the presence of native TiO_2 and metallized TiO_2 suspensions. Part (II): photocatalytic mechanism. Water Res 1999;33:669–76.

[7] Dickinson A, James D, Perkins N, Cassidy T, Bowker M. The photocatalytic reforming of methanol. J Mol Catal A 1999;146:211–21.

[8] Ichikawa S. Chemical conversion of carbon dioxide by catalytic hydrogenation and room temperature photo-electocatalysis. Energy Convers Manage 1995;36:613–6.

[9] Adachi A, Ohta K, Mizuno T. Photocatalytic reduction of carbon dioxide to hydrocarbon using copper-loaded titanium dioxide. Solar Energy 1994;53:187.

[10] Tseng IH, Chang WC, Wu JCS. Photoreduction of CO_2 using sol–gel derived titania and titania-supported copper catalysts. Appl Catal B Environ 2002;37:37–48.

[11] Tseng IH, Wu JCS, Chou HY. Effects of sol–gel procedures on the photocatalysis of Cu/TiO_2 in CO_2 photoreduction. J Catal 2004;221:432–40.

[12] Sakata Y, Yamamoto T, Okazaki T, Imamura H, Tsuchiya S. Generation of visible-light response on the photocatalyst of a Cu ion containing TiO_2. Chem Lett 1998; 1253–4.

[13] Tauc J. In: Tauc J, editor. Amorphous and liquid semiconductors. NY: Plenum; 1974. p. 159–220.

[14] Wang Y, Suna A, Mahler M, Kasowski R. PbS in polymers—from molecules to bulk solids. J Chem Phys 1987; 87:7315–22.

[15] Kosacki I, Petrovsky V, Anderson HU. Band gap energy in nanocrystalline ZrO_2:16%Y thin films. Appl Phys Lett 1999;74:341–3.

[16] Wagner CD, Davis LE, Zeller MV, Taylor JA, Raymond RM, Gale LH. Empirical atomic sensitivity factors for quantitative analysis by electron spectroscopy for chemical analysis. Surf Interface 1981;3:211–25.